Sensitivity of satellite microwave and infrared observations to soil moisture at a global scale: Relationship of satellite observations to in situ soil moisture measurements

Catherine Prigent,[1] Filipe Aires,[2,3] William B. Rossow,[4] and Alan Robock[5]

Received 3 June 2004; revised 5 October 2004; accepted 19 January 2005; published 13 April 2005.

[1] This study presents a systematic and integrated analysis of the sensitivity of the available satellite observations to in situ soil moisture measurements. Although none of these satellites is optimized for land surface characterization, before the launches of the SMOS- and HYDROS-dedicated missions they are the only potential sources of global soil moisture measurements. The satellite observations include passive microwave emissivities, active microwave scatterometer data, and infrared estimates of the diurnal amplitude of the surface skin temperature. The Global Soil Moisture Data Bank provides in situ soil moisture measurements in five separate regions. This simultaneous analysis of various satellite observations and the large amount of in situ measurements has two major advantages. First, this analysis helps identify and separate the physical mechanisms that affect the satellite observations. For example, we show that the passive microwave polarization differences at 19 GHz and above are essentially sensitive to the vegetation and not to the soil moisture (i.e., the correlation between microwave observations and soil moisture is only indirect and comes from the statistical correlation between vegetation and soil moisture). Second, this analysis enables an objective comparison of the relative potential of the various satellite observations for soil moisture retrieval when other conditions are held constant. The second part of this study benefits from this synthesis to derive a relationship between satellite observations and soil moisture at a global scale.

Citation: Prigent, C., F. Aires, W. B. Rossow, and A. Robock (2005), Sensitivity of satellite microwave and infrared observations to soil moisture at a global scale: Relationship of satellite observations to in situ soil moisture measurements, *J. Geophys. Res.*, *110*, D07110, doi:10.1029/2004JD005087.

1. Introduction

[2] Soil moisture only amounts to less than 1/10,000 of the total water on the planet. Nevertheless, it strongly affects surface energy and water exchanges at the land-atmosphere interface and it represents the main source of water for agriculture and natural vegetation. Soil moisture is a very important variable for a large range of applications at various spatial and temporal scales, from climate and weather predictions to agriculture, water management, or flood monitoring.

[3] However, in situ measurements of soil moisture are not performed on a routine basis. In addition, the representativity of point measurements for regional applications is often questioned. Quality measurements in agricultural regions from a variety of climates have recently been grouped into a data bank [*Robock et al.*, 2000], partly to evaluate the temporal and spatial scales of the soil moisture variability.

[4] The only soil moisture estimates available at a global scale are derived from land surface models, but these models face numerous challenges. They are very sensitive to the parameterizations of the complex processes involved. They suffer from uncertainties in the atmospheric forcing and lack information on key parameters like the soil texture. And last but not least, they suffer from the absence of adequate observations to evaluate the outputs, especially the surface skin temperature and soil moisture. During the Atmospheric Model Intercomparison Project (AMIP) in 1994, 30 soil moisture fields were compared, based on models ranging from simple so-called bucket schemes to more complex ones but it was very difficult to separate the effects of erroneous forcing from a lack of realism in the modeling [*Robock et al.*, 1998]. Recent comparison of the

[1]Laboratoire d'Etudes du Rayonnement et de la Matire en Astrophysique, Centre National de la Recherche Scientifique, Observatoire de Paris, Paris, France.
[2]Department of Applied Physics and Applied Mathematics, Columbia University, NASA Goddard Institute for Space Studies, New York, New York, USA.
[3]Also at Laboratoire de Météorologie Dynamique, Centre National de la Recherche Scientifique, Institut Pierre-Simon Laplace, École Polytechnique, Palaiseau, France.
[4]NASA Goddard Institute for Space Studies, New York, New York, USA.
[5]Department of Environmental Sciences, Rutgers University, New Brunswick, New Jersey, USA.

Copyright 2005 by the American Geophysical Union.
0148-0227/05/2004JD005087

revised versions of six of these models did not show significant improvements in soil moisture estimates [*Srinivasan et al.*, 2000]. Even when forced with the same meteorological observations, the model runs for a two year period during the Global Soil Wetness Project (GSWP) compared poorly with the actual in situ soil moisture measurements. Recent works include *Li et al.* [2005]; however, once corrected for region-dependent biases, these models reproduced rather satisfactorily the seasonal cycle of soil moisture [*Entin et al.*, 1999]. As *Douville et al.* [1999, p. 305] pointed out, soil moisture is "one of the most difficult climatological parameters to model and . . . any computed climatology must be considered with caution."

[5] A large number of studies have addressed the possibility of retrieving soil moisture from satellite observations both in the infrared (IR) and microwave (MW) domains. The thermal and dielectric properties of water are very different from other natural surfaces and as a consequence, the presence of water in soil drastically modifies the properties measured in the thermal IR and in the MW domain. *Schmugge et al.* [1980] give a detailed description of the basic principles of remote sensing of soil moisture in the IR and MW and a review of the pioneering work.

1.1. Soil Moisture Retrievals From Satellite Infrared Measurements

[6] The amplitude of the diurnal cycle of surface skin temperature (T_s) is related to external factors (incident solar radiation, air humidity and temperature, wind) and to surface characteristics (vegetation, thermal conductivity C, and heat capacity K, often combined into the thermal inertia $P = (KC)^{1/2}$). With increasing soil moisture, the thermal inertia increases, meaning that changes in T_s related to a given change in incident solar flux decrease. For moist soil, evaporation reduces the net energy to the soil. As a consequence, when the surface is moister, the temperature is driven by evaporation, whereas when the surface is drier, thermal inertia is the dominant driver so that the amplitude of the T_s diurnal cycle is related to the soil moisture at the surface.

[7] Several studies have examined the relationship between soil moisture and T_s measurements. Some approaches use two measured temperatures, one at midday and the other close to midnight, while others suggest that a single temperature is enough [*Taconet et al.*, 1986]. *Wetzel et al.* [1984] studied the diurnal surface temperature cycle to identify the signatures in that cycle that are the most sensitive to soil moisture and found that the midmorning rate of increase is the best predictor. More recent studies couple T_s measurements and vegetation indices, such as the Normalized Difference Vegetation Index (NDVI), for better control of the respective soil and vegetation contributions [*Gillies and Carlson*, 1995; *Goetz*, 1997], along with increased use of complex land surface transfer models [*Friedl*, 1995]. A special issue of *Remote Sensing of the Environment* [*Goetz*, 2002 and the following papers] is dedicated to recent advances in this domain. One key problem in using satellite estimates of T_s for soil moisture retrieval is related to the limited time sampling of the measurements, which hampers analysis of the full diurnal cycle of T_s. *Jin* [2004], for example, uses model-based assumptions about the diurnal cycle in combination with twice daily satellite measurements to recover T_s, but these data could not be used to infer soil moisture variation. Instead, direct determination of the full diurnal cycle of T_s is needed, independent of model assumptions.

1.2. Soil Moisture Estimates From Satellite Passive and Active Microwave Measurements

[8] Water has a very large dielectric constant as compared to other natural substances and this translates into specific responses at both active and passive MW frequencies. However, the signal from moist soil is modulated by surface roughness, vegetation canopy, and atmospheric absorption. The lower the microwave frequency the smaller these effects. In addition, the penetration depth of MW radiation within the soil, also referred to as the thermal sampling depth, is defined as the inverse of the soil extinction coefficient and is generally of the order of a wavelength. As a consequence, frequencies over 10 GHz cannot provide information from below the very first cm of the soil surface, especially when the soil is moist; the lower the frequency, the more sensitive to a larger depth below the subsurface.

[9] In addition to research using aircraft and crane-mounted instruments [e.g., *Calvet et al.*, 1996], many studies are devoted to the use of passive microwave satellite observations for soil moisture retrieval with observations that are today available. The most recent works are briefly reviewed here. From analysis of Scanning Multichannel Microwave Radiometer (SMMR) data and collocated in situ soil moisture measurements in Illinois, *Vinnikov et al.* [1999] showed that frequencies up to 18 GHz have a real potential for soil moisture monitoring at least in areas with small vegetation density. Surprisingly, they observe similar sensitivity to soil moisture at 18 GHz and 6 GHz. They clearly mention in this study that part of the correlation to soil moisture could be related to variations in the vegetation and that these effects are not easy to separate. *Reichle et al.* [2004] compare soil moisture estimates from SMMR, modeled soil moistures, and in situ measurements, for nine years all over the globe. They conclude that time average fields from the model and the satellite agree well but that the magnitude and variability of the soil moisture estimates are very different. They point out that local bias correction or rescaling might be necessary before assimilation of the satellite data into land surface models. From observations with the Tropical Rainfall Measurement Mission (TRMM) Microwave Instrument (TMI), during the Southern American Great Plains (SGP99) experiment, *Jackson and Hsu* [2001] concluded that the 10 GHz frequency provides new information on soil moisture. On the basis of temporal changes, *De Ridder* [2003] inferred soil moisture from Special Sensor Microwave/Imager (SSM/I) data only and showed a reasonable dynamical agreement between the soil moisture estimate and precipitation, in rather sparsely vegetated areas in Europe. *Wen and Su* [2003] developed an algorithm from the three lower frequency channels of TMI (10, 19, and 21 GHz) to retrieve the surface skin temperature and soil moisture and obtained a correlation of 0.82 between estimated and in situ soil moisture measurements over Tibet. More and more studies couple soil-vegetation-atmospheric models and satellite observations to help solve the soil moisture problem by using various relationships between surface variables and satellite observations. *Lakshmi et al.* [1997] used a land-atmosphere

model and a radiative transfer code to simulate soil moisture and MW responses. Comparison between SSM/I observations and simulation showed a promising agreement when averaged over a month and the monthly estimates of the evaporation derived from the SSM/I measurement also compared satisfactorily with the modeled atmospheric estimates. However, at frequencies at and above 19 GHz, modulation of the passive MW signal by vegetation and surface temperature can be significant and several studies have exploited it to characterize the vegetation [e.g., *Choudhury and Tucker*, 1987; *Choudhury*, 1989; *Prigent et al.*, 2001] or to retrieve the surface temperature from multifrequency MW observations [*McFarland et al.*, 1990; *Njoku*, 1995; *Basist et al.*, 1998; *Aires et al.*, 2001].

[10] Many satellite studies on active microwave have focused on Synthetic Aperture Radar (SAR) data from European Research Satellite (ERS) for their high spatial resolution suitable for agricultural or small-scale hydrology applications [e.g., *Quesney et al.*, 2000; *Moran et al.*, 2000]. The major issue in these studies was to subtract the roughness or vegetation effects using change-detection methods or by modeling their contributions. The methods were applied to limited areas so their extension to larger regions is questionable. At a larger scale, using the ERS wind scatterometer data at 5.25 GHz, *Woodhouse and Hoekman* [2000a, 2000b] estimated soil moisture with an inversion method that incorporates both modeling and a priori quantitative information. *Wagner et al.* [1999a, 1999b] developed a methodology to retrieve soil moisture from the same instrument, based mainly on a change-detection methodology. They produce a global soil moisture data base that they compare to precipitation data and to land surface model outputs [*Wagner et al.*, 2003].

[11] Active microwave observations have often been thought to be more sensitive to surface roughness and vegetation and less to soil moisture than passive MW. *Schmugge et al.* [2002] did not consider active MW as a promising tool for soil moisture detection, although *Du et al.* [2000] used simulations at 1.5 GHz to conclude that as far as vegetation is concerned, neither sensor type is superior to the other. This question is still being debated. The solution might be to exploit more fully the complementarity of the two modes to extract soil moisture information, as already suggested by campaign experiments.

[12] Efforts now focus on the development of MW instruments at low frequencies. The 1.4 GHz band appears to be optimal for soil moisture detection, because of its lower sensitivity to soil roughness and vegetation and its larger penetration depth. However, adequate spatial resolution cannot be obtained with conventional antennas of a reasonable size. The European SMOS (Soil Moisture and Ocean Salinity) project to be launched in 2007 [*Kerr et al.*, 2001] will fill the gap, providing ~50 km spatial resolution from 1.4 GHz passive measurements, thanks to interferometric antenna designs. The US HYDROS mission, planned for launch in 2010, will provide soil moisture measurements from L-band observations in both passive and active modes [*Entekhabi et al.*, 2002].

1.3. New Approach

[13] No satellite sensor today has optimal characteristics for soil moisture retrieval. The frequencies and the spatial and temporal resolutions have not been specifically selected for continental studies. The ERS scatterometer for instance was designed to measure wind speed over ocean, and SSM/I retrieval algorithms mainly focus on atmospheric and ocean analysis. Continental applications are often only by-products of these satellite observations. Dedicated missions like SMOS or HYDROS will not be launched for several years, and before these missions collect enough observations for climatological purposes, at least 10 years will have passed. Land surface model intercomparison groups are now producing soil moisture estimates. The second initiative of the GSWP is one example. They express the need for consistent global data sets to evaluate their outputs [*Entin et al.*, 1999]. What can be done today with the available observations?

[14] The objective of this study is to investigate the sensitivity of all available satellite observations related to soil moisture on a global basis, to analyze their complementarity, and to assess the ability of combinations of these satellite measurements for soil moisture estimation. Our results provide a synthesis of the previous separate studies that examined one instrument or one wavelength at a time. We only consider observations that have been available for at least 10 years on a regular basis all over the globe, with spatial resolutions that are compatible with climate analysis. The observations include the three types of measurements that have been shown sensitive to soil moisture: thermal infrared, and passive and active microwaves. For each type of observations, the optimum products are selected. The thermal infrared observations come from both the NOAA polar orbiters and the geostationary meteorological satellites, as processed by the International Satellite Cloud Climatology Project [*Rossow and Schiffer*, 1999] to obtain direct determination of the diurnal cycle of land surface skin temperature [*Aires et al.*, 2004]. Passive MW information is provided by the SSM/I from which the MW land surface emissivities have been calculated; this analysis separates the T_s and emissivity contributions to the observed signal, unlike previous studies [*Prigent et al.*, 1997, 1998]. The active MW observations are extracted from the ERS scatterometer. In addition, the Advanced Very High Resolution Radiometer (AVHRR) combining visible and near infrared reflectances (NDVI) is used to help quantify and eventually separate the vegetation contribution from the other factors. The in situ measurements from the Global Soil Moisture Data Bank [*Robock et al.*, 2000] are the primary source of data for comparison. However, given the limited spatial coverage of this data bank, the reanalayses from the National Centers for Environmental Prediction (NCEP) and the European Centre for Medium-Range Weather Forecasting (ECMWF) numerical weather prediction (NWP) models will also be examined in the second part of this study. The soil moisture in situ measurements and the satellite observations are described in section 2. Section 3 presents the comparison between these data sets with special emphasis on the ambiguity between the vegetation and the soil moisture signatures in the satellite observations. Section 4 concludes the first part of this study.

2. Data Sources

[15] The data sets cover a large range of sources from in situ measurements, satellite observations, and model outputs, each one being available for a given time period and

Table 1. In Situ Measurement Characteristics Used in This Study[a]

Region	Stations	Surface Type	Frequency	Period	Depth, cm
Illinois	19	mostly grass	1–3/month	all year	10
Iowa	6	corn	2/month	growing season	7.8
Russia	171	cereal crops	every 10 days	all year	20
India	11	grass	1/week	all year	~10
Mongolia	42	pasture and wheat	every 10 days	spring and summer	10

[a]From *Robock et al.* [2000].

having its own space and time resolution. Since ERS data are available since the end of 1991 but several in situ soil moisture stations are not available after 1995, the years 1993 and 1994 have been selected for the comparison. These two years are also part of the GSWP2 initiative, making this work useful in the GSWP2 framework. Comparisons between satellite and point measurements are often suspected because of the differences in spatial and temporal scales. Very small-scale spatial and temporal variations of soil moisture are related to topography, soil texture, and vegetation. This small scale variability is very difficult or even impossible to model and *Robock et al.* [2000] describe it as a stochastic process. In addition the large variability on scales of order of 1–2 months and 500 km has been extracted from dense networks of in situ measurements, at least at midlatitudes [*Vinnikov et al.*, 1996; *Robock et al.*, 2000; *Entin et al.*, 2000]. Since this variability is attributed to atmospheric forcing, it can be modeled. Our study will focus on the analysis of the large scale variability of the soil moisture, compatible with typical satellite resolution of the order of a few tens of kilometers, averaged on a monthly basis.

[16] In situ measurements are available at different depths in the subsurface and NWP models also calculate the soil moisture for specific subsurface layers, whereas the selected satellite observations are sensitive, at best, to the first few centimeters of the surface. In this study, the soil moisture is defined as the total volumetric soil moisture, i.e., the volumetric percent of water in the first 10 cm. Unfortunately, depending on the data set, the soil layers considered are not equivalent, the first layer ranging from 5 cm to 20 cm. We verified using the in situ measurements from the Global Soil Moisture Data Bank that the soil moisture variations between 5 and 20 cm are highly correlated. The satellite data we will use are essentially sensitive to the surface top (the penetration depth is usually of the order of the observed wavelength). We checked on ancillary data sets providing a detailed description of the vertical soil moisture profiles [*Calvet et al.*, 1999; *Wigneron et al.*, 1995] that the surface top moisture (~0.5 cm) is rather well correlated with the 10 cm layer moisture, even at small timescales (correlation of at least 0.6 for the 4 analyzed locations with daily measurements). When averaged over the month, even larger correlations are expected.

[17] Most satellite observations (the ERS backscattering, the SSM/I emissivities, and the AVHRR NDVI) have already been described in detail in the work of *Prigent et al.* [2001] and are summarized below. The variables are all mapped on an equal area grid with a spatial resolution of 0.25° at the equator.

2.1. In Situ Measurements From the Global Soil Moisture Data Bank

[18] The Global Soil moisture Data Bank [*Robock et al.*, 2000] is a collection of in situ soil moisture measurements from ~600 stations in the Northern Hemisphere, mostly in agricultural areas, spanning ~40 years of data for some stations. At most stations, gravimetric techniques are used at several depths in the subsurface, every ~10 days, but only during spring and summer seasons in some areas. Possible applications of this data set are three-fold: to analyze the spatial and temporal scales of variation of the soil moisture, to evaluate land surface models, and to assess remote sensing methods. Unfortunately, several stations do not provide measurements after 1990. All the measurements available for 1993 and 1994 are examined in this study, and their characteristics are summarized in Table 1. As already mentioned, only the top layer measurements are used. These in situ measurements come from various locations: Russia [*Robock et al.*, 1995; *Vinnikov and Yeserkepova*, 1991; *Vinnikov et al.*, 1996], Mongolia [*Entin et al.*, 2000; *Robock et al.*, 2000], India [*Robock et al.*, 2000], Iowa [*Entin et al.*, 2000], and Illinois [*Hollinger and Scott*, 1994]. These regions represent a large range of soil moisture behaviors. The Russian and American stations are characterized by wet winters and rather dry summers. The Indian region is dominated by the summer monsoon, which produces a large amplitude soil moisture variation, with wet summers and dry winters. In contrast, the stations in Mongolia show very stable soil wetness during the year (measurements stopped at the end of 1993). Point measurements without averaging or gridding are compared to the closest satellite observations.

2.2. Active MWs: ERS Scatterometer Backscattering at 5.25 GHz

[19] The ERS scatterometer operates at 5.25 GHz vertical polarization with a 50 km spatial resolution. Primarily designed for ocean applications, the scatterometer observations have also shown potential for land surface characterization [e.g., *Frison and Mougin*, 1996a; *Wismann et al.*, 1996; *Wismann*, 1999]. The backscattering signal is measured by three antennas, one looking normal to the satellite flight path and the other two pointing 45° forward and backward, with viewing angles ranging from 18° to 59°. The scatterometer response is very stable over time for constant targets; the measurement uncertainty is estimated to be about 5%. Atmospheric absorption and emission are negligible at 5.25 GHz and no correction is required. Good antenna intercalibration enables the use of all three antennas.

[20] For a given location, variation of the scattering signal with incidence angle is the dominant source of variability [*Messeh and Quegan*, 2000]. Azimuth angle effects are small over vegetated surfaces, although anisotropic signatures have been observed over some deserts [*Frison and Mougin*, 1996a; *Messeh and Quegan*, 2000]. *Frison and Mougin* [1996b] compared the scatterometer responses at

various incidence angles and showed that the radar signal at low incidence angles ($\leq 20°$) is related to soil characteristics, whereas observations at large incidence angles ($\sim 45°$) provide more information about vegetation. From a similar analysis, *Wagner et al.* [1999a, 1999b] found that the backscattering coefficient was sensitive to soil moisture over the whole incidence angle range in moderate-density vegetation areas and recommended examination of the slope of the angular dependence for vegetation analysis. However, as this slope parameter is very sensitive to noise, several years of data are required to calculate it, making its use for determining variations less valuable.

[21] In this study, for incidence angles below and above 30° respectively, the scatterometer response is approximated by a linear function of the incidence angle and the fitted values at 20° and 45° are kept, following a method similar to *Frison and Mougin* [1996a]. *Messeh and Quegan* [2000] tested several incidence angle models and found that none was adequate globally. By separating the angle values into two and using a simple linear regression model on each range, we can test and possibly help separate the soil moisture and vegetation contributions. For a moderate-density vegetation cover, the backscattering coefficient increases in theory with soil moisture increases for both incidence angle ranges, but at a lower rate for the larger angles. For both angle ranges, this coefficient increases with increasing vegetation density as well.

2.3. Passive MWs: SSM/I Emissivities Between 19 and 85 GHz

[22] The SSM/I instruments on board the Defense Meteorological Satellite Program (DMSP) polar orbiters observe the Earth twice daily at 19.35, 22.235, 37.0, and 85.5 GHz with both vertical and horizontal polarizations, with the exception of 22 GHz which is vertical polarization only. The observing incidence angle is close to 53° and the fields of view decrease with frequency, from 43 km × 69 km to 13 km × 15 km [*Hollinger et al.*, 1987]. In our analysis, MW emissivities of land surfaces are estimated from SSM/I observations by removing contributions from the atmosphere, clouds, rain, and the surface temperature using ancillary data from the International Satellite Cloud Climatology Project (ISCCP) [*Rossow and Schiffer*, 1999] and the NCEP reanalysis [*Kalnay et al.*, 1996]. Cloud-free SSM/I observations are first isolated using collocated visible/ infrared satellite observations (ISCCP data). The cloud-free atmospheric contribution is then calculated from an estimate of the local atmospheric profile from NCEP reanalysis. Finally, with the surface skin temperature derived from IR observations (ISCCP estimate), the surface emissivity is calculated for the seven SSM/I channels [*Prigent et al.*, 1997, 2001]. The standard deviations of the day-to-day variations of the retrieved emissivities within a month are typically about 0.012 for all the SSM/I frequencies, which is an estimate of the accuracy of these emissivities.

[23] In contrast to the direct use of the MW brightness temperatures for surface characterization, the calculated emissivities are related to the surface properties themselves without confusing signals from atmospheric contribution or surface temperature variations. At 53° incidence, theory indicates that, at a given frequency, the MW emissivity decreases with increasing soil moisture and the emissivity difference between the two linear polarizations increases. Increasing vegetation density has the opposite effect.

2.4. Thermal Infrared: The Diurnal Amplitude of T_s Normalized by the Incident Shortwave Flux

[24] The land surface skin temperature T_s, which is not conventionally observed at meteorological weather stations, can be estimated from satellite infrared observations. The most extensive data set of land skin temperature is produced at 3 hour intervals since 1983 over the globe, every 30 km, by ISCCP [*Rossow and Schiffer*, 1999]. It combines all the infrared measurements from polar and geostationary operational weather satellites. Recently *Aires et al.* [2004] obtained the complete diurnal cycle of the surface skin temperature based on the global ISCCP 3 hourly T_s estimates for clear scenes over a year. They developed a method to reconstruct the complete daily T_s diurnal cycle at each location over the globe, based on a statistical analysis of the data sets and excluding model calculations. Once the full diurnal cycle of surface skin temperature is known, an accurate determination of its amplitude during the day is derived. For a given diurnal heat flux variation, the amplitude of the surface temperature variation is inversely proportional to the thermal inertia which increases with soil moisture. The amplitude of the surface temperature is related to the soil moisture, both through its effect on the thermal inertia and through its control of evaporation. To account for the dependence of the diurnal amplitude of T_s with cloud-induced variations of the solar insulation, the T_s amplitudes are normalized by the shortwave net fluxes at the surface. Surface radiative fluxes have been determined by *Zhang et al.* [2004] using radiative transfer modeling and ancillary data sets to specify the Earth's atmosphere and surface. Uncertainties on the monthly mean fluxes are of the order of 10 W/m^2 globally.

[25] For a finer temporal resolution of the characterization of soil moisture, the diurnal cycle of the surface skin temperature should be reconstructed not only for clear sky but also for cloudy cases. *Aires et al.* [2001] developed an algorithm to retrieve surface skin temperature in cloudy scenes using the SSM/I MW information. In this study, only monthly timescales are considered, so no cloudy surface skin temperature diurnal cycles are considered at this stage but the shortwave flux normalization accounts for the average cloud effects.

2.5. Ancillary Vegetation Information

[26] The NDVI, calculated from the red and near-infrared channels of AVHRR, is extensively used for vegetation studies. The availability of NDVI data for two decades and its high horizontal spatial resolution have motivated a large number of studies from regional to global scales [e.g., *Tucker et al.*, 1985; *DeFries et al.*, 1999]. The NDVI has been found to be correlated with the fraction of photosynthetically active radiation absorbed by green vegetation and the leaf area index [e.g., *Begue and Myneni*, 1996], as well as providing information about vegetation phenology [*Moulin et al.*, 1997]. However, the sensitivity of this parameter to satellite intercalibration, zenith angle drifting, or cloud contamination has often been mentioned [e.g., *Gutman*, 1999; *Tanré et al.*, 1992], so NDVI should be

Table 2. Expected Sign of the Correlation Between the Satellite Observations and Two Surface Parameters

Observation Type	Variable	Soil Moisture	Vegetation Density
Passive microwave	emissivity polarization difference	positive	negative
	emissivity vertical polarization	negative	negative
	emissivity horizontal polarization	negative	positive
Active microwave	backscattering coefficient small angles	positive	depends
	backscattering coefficient large angles	depends	positive
Thermal infrared	T_s diurnal amplitude (normalized or not)	negative	negative

used with care. In this study, the NDVI will help analyze the vegetation contribution in the other satellite observations.

2.6. Summary

[27] Table 2 summarizes the observations used in this study and how the major surface parameters contribute to the signals, namely the soil moisture and the vegetation.

[28] Snow can also significantly change the observed satellite signals, but this contribution will not be examined here (we use the NOAA operational snow product to eliminate snow covered locations from consideration). As mentioned earlier, both vegetation and soil moisture increases result in similar responses of the active MW and T_s diurnal amplitude. In contrast, these increases have opposite effects on the passive MW emissivities and polarization difference.

[29] Figure 1 displays a monthly mean map (July 1993) for each satellite observation type: the emissivity polarization difference at 19 GHz and 53° incidence angle for passive microwaves, the backscattering coefficient at 5.25 GHz interpolated to 45° for active microwaves, and the amplitude of the diurnal cycle of T_s extracted from thermal IR observations. It is worth noting that the amplitude of the diurnal cycle is not available over Central Asia or at higher latitudes, where geostationary satellite coverage is lacking.

3. Analysis of the Collocated In Situ and Satellite Measurements

[30] We used soil moisture data from 249 stations. The locations of the in situ measurement stations are indicated on Figure 1, bottom map. All the satellite variables are gridded the same way, for each map grid the in situ measurements that are located within it are averaged. Most stations are far enough apart that they fall into separate grid points, except in Iowa where all the stations are grouped in a very small region. For each region, the following numbers of satellite grid locations are considered: 17 in Illinois, 1 in Iowa, 125 in Russia, 9 in India, and 18 in Mongolia.

3.1. General Analysis

3.1.1. Soil Moisture and Vegetation Sensitivity

[31] Figure 2 (left) presents the scatterplots of the various monthly mean satellite measurements and the coincident near surface in situ soil moisture measurements for all the locations over the two year period, avoiding the snow season.

[32] For the passive MW, the polarization differences at 19 and 37 GHz were used, along with the individual polarizations at 19 GHz. The backscattering coefficients from ERS for both small and large incidence angles are used. The infrared information is given by the T_s diurnal amplitude along with the same variable normalized by the average solar insulation. The different regions are indicated by different symbols and for each scatterplot, the linear correlation coefficient is indicated. For all the satellite observations, there is a considerable scatter in the data. Table 3 summarizes the correlation coefficients, totally and for each region separately.

[33] When considering all the coincident measurements, the correlation coefficients are very low except for the active MW observations (Table 3). Depending on the region, the correlations between the soil moisture and the satellite observations vary a lot, even changing sign for a given instrument from one region to another. For instance, there is a positive correlation between the passive MW polarization difference and the soil moisture in Illinois but a negative one in Mongolia. At 19 and 37 GHz, the correlation coefficients are surprisingly similar. We also calculated them for 85 GHz and they are also comparable (not shown). Note that the NDVI exhibits a similar low correlation with soil moisture, including puzzling regional sign changes. The largest correlation and the most stable one from one region to another was obtained with the active MW at small incidence angle. Part of the scatter between the satellite estimates and the in situ soil moisture measurements is likely related to the mismatch of spatial resolution. The comparison involves point measurements with satellite observations that are integrated over a pixel that is representative of roughly 25 km × 25 km. As shown by *Entin et al.* [2000], the small-scale soil moisture variance accounts for ~30–80% of the total variance. Although this spatial resolution issue inevitably reduces the correlation between the satellite estimate and the point measurement, it alone cannot explain the unexpected changes of sign in the correlations between the in situ measurements and the satellite observations for the passive MW in some regions.

[34] Figure 2 (right) and the corresponding Table 4 contain similar information as Figure 2 (left) and Table 3, but for the relationships with the vegetation information in the NDVI. The correlations are much higher and almost always with the expected sign (see Table 2), whatever the instrument [*Prigent et al.*, 2001]. In addition, responses from one region to another are more stable.

3.1.2. Local Standardization

[35] From one location to another, the satellite observations are affected by different sources of variability in different ways, the soil moisture and the vegetation being the two major contributors but not the only ones. At a given location, there is a reduced number of sources of variability and the correlation between the in situ soil moisture measurements and the satellite observations is generally larger. In order to examine the sensitivity of the satellite measurements to soil moisture more closely, the correlations have been recalculated, subtracting for each observation and each location the mean value over the two years and normalizing them by

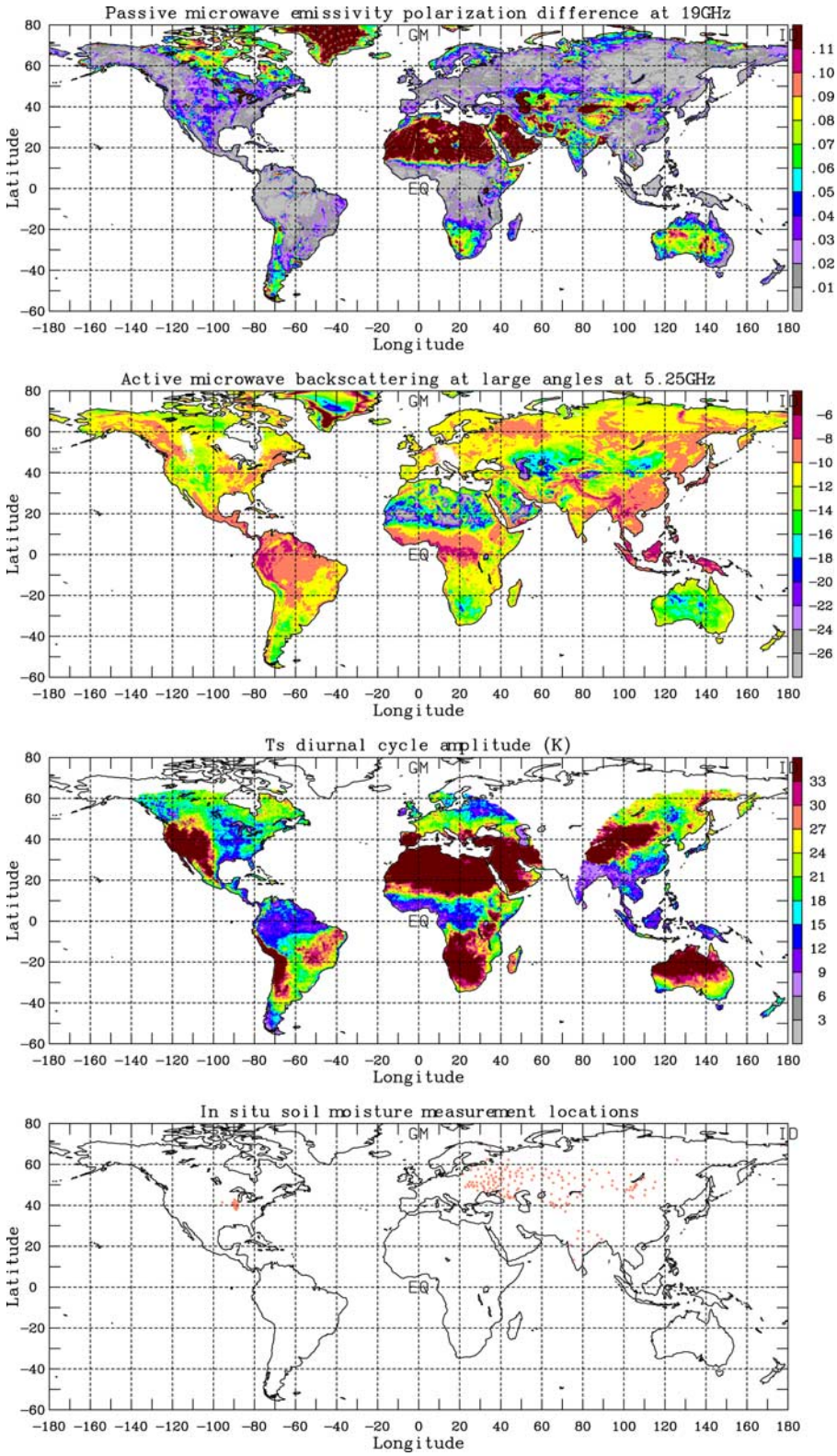

Figure 1. Examples of global monthly mean satellite variables for July 1993 and locations of the in situ measurement stations. From top to bottom: Passive microwave SSM/I emissivity polarization difference at 19 GHz, active microwave ERS backscattering for large incidence angle, Ts diurnal amplitude derived from infrared measurements, and location of the in situ soil moisture measurement stations.

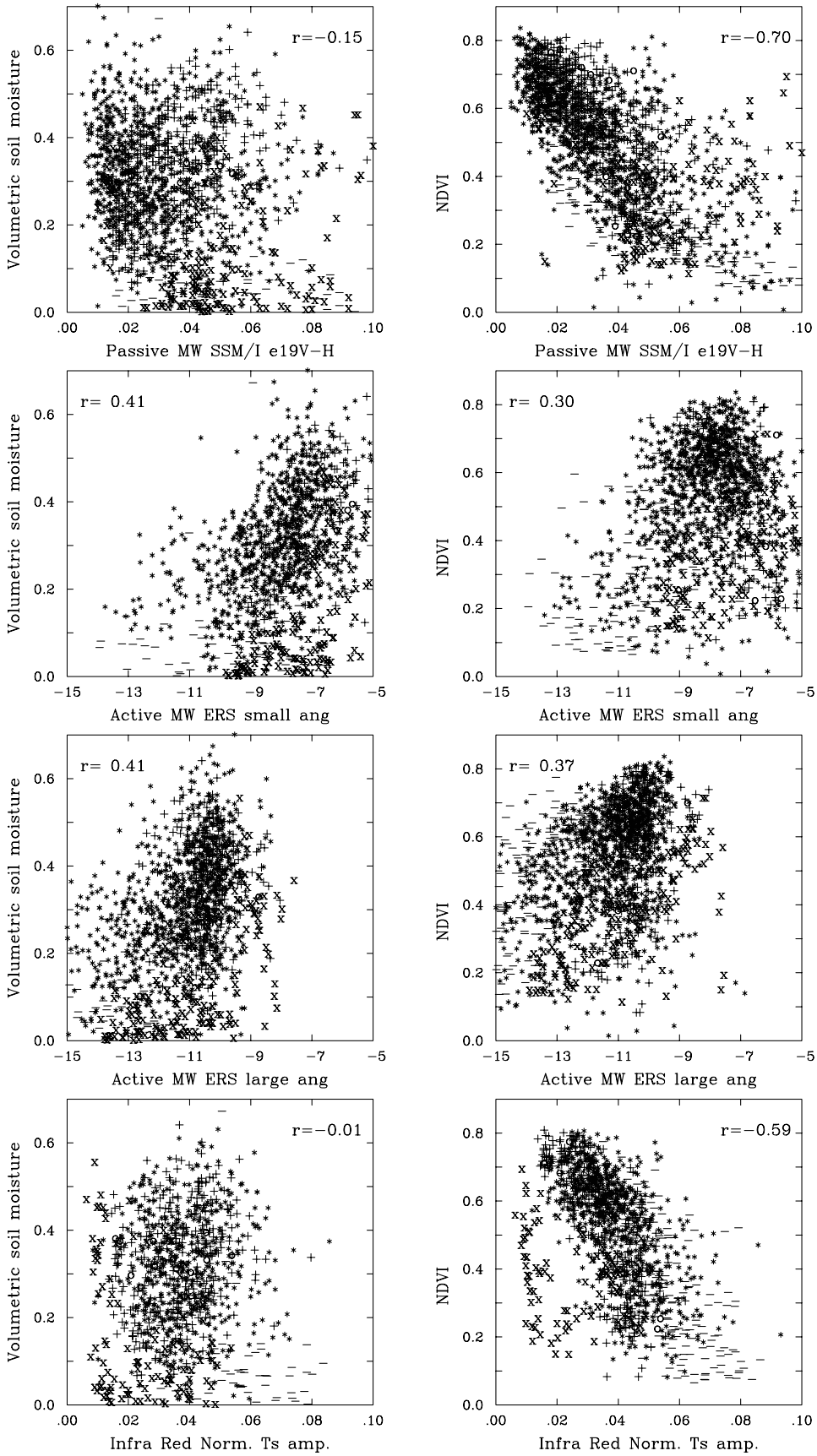

Figure 2. Scatterplots of the satellite derived products (left) versus in situ soil moisture measurements and (right) versus the NDVI observations. For each scatterplot the linear correlation is indicated. Symbols represent each region: pluses, Illinois; circles, Iowa; asterisks, Russia; crosses, India; dashes, Mongolia.

Table 3. Linear Correlation Coefficients Between the In Situ Soil Moisture and the Satellite Measurements

Variables	Total	Illinois 17 Sites	Iowa 1 Site	Russia 125 Sites	India 9 Sites	Mongolia 18 Sites
Passive MW SSM/I e19V-H	−0.15	0.43	0.18	−0.13	0.03	−0.32
Passive MW SSM/I e37V-H	−0.12	0.40	0.26	−0.13	0.16	−0.35
Passive MW SSM/I e19V	−0.02	−0.22	−0.25	0.03	−0.30	−0.03
Passive MW SSM/I e19H	0.07	−0.39	−0.27	0.09	−0.16	0.28
Active MW ERS small angles	0.41	0.51	0.36	0.45	0.52	0.14
Active MW ERS large angles	0.41	0.00	−0.04	0.43	0.58	−0.07
IR Ts amplitudes	−0.17	0.03	0.08	−0.10	−0.42	−0.19
IR normalized Ts amplitudes	−0.01	0.23	0.17	0.02	−0.28	−0.30
NDVI vegetation	0.18	−0.46	−0.23	−0.07	0.46	0.28

the standard deviation in the given observations for that location (Table 5). This process is called "local standardization," which has the effect of partly suppressing the variability that is location-dependent. This fact explains why some local soil moisture retrieval schemes work well, even if they use only a single source of satellite information. Applying these algorithms globally would inevitable fail because additional, geographically specific sources of variability are not taken into account. Our goal is to develop general soil moisture retrieval algorithms that suppress the impact of vegetation and other surface parameter differences.

[36] For the passive microwaves and the active microwaves with small incidence angle, the correlations between in situ measurements and the satellite observations that are locally standardized are larger and show the expected signs (except in Mongolia). This suggests that if the sensitivity of the satellite observations to the various interacting factors (e.g., soil moisture, vegetation, soil texture, and roughness) is different, it might be possible to exploit these different sensitivities by analyzing all the satellite observations together.

[37] This argument introduces two distinct types of soil moisture variability. The first one, at a larger scale, is dependent on several local parameters, that explain site-to-site variations and require multiple satellite observation sources to characterize them. This large-scale variability will be investigated in a companion paper. The other type of soil moisture variability is more localized and can be assessed more easily once the mean local soil moisture state is known. This source of variability makes localized retrieval schemes possible: these schemes work on soil moisture anomalies instead of absolute values. In the following, this localized and smaller-scale soil moisture variability is analyzed together with the satellite observations.

3.2. Regional Analysis

[38] To further investigate the mechanisms that drive the relationship between satellite observations and in situ soil measurements, for each region (except for the Iowa sites, which cover too limited an area), one time series for each variable and for the two years is presented along with precipitation data from the Global Precipitation Climatology Project (GPCP) [*Huffman*, 1997] (Figures 3a–3d). For each variable and each location, the correlation coefficients are indicated in Table 6. Illinois, Iowa, and Russia belong to similar climate zones and will be discussed together.

3.2.1. Illinois, Iowa, and Russia

[39] The in situ measurement stations presented in Illinois and Russia have a typical midlatitude seasonal cycle with wet winters and dry summers (Figures 3a and 3b). The ECMWF and NCEP soil moisture estimates exhibit a much weaker annual cycle compared to the in situ measurements. GPCP precipitation estimates do not show a marked annual cycle either. The vegetation density reaches its maximum during summer (see the NDVI in Figures 3a and 3b), giving rise to a strongly negative correlation between the in situ soil moisture and the vegetation. For both cases, the SSM/I polarization difference increases with soil moisture as predicted and decreases with vegetation density with significant correlation coefficients. The ERS backscattering coefficient for large angles reacts as expected to vegetation density. For low incidence angles, the backscattering coefficient increases with soil moisture as predicted and is not very sensitive to vegetation density. The normalized T_s diurnal amplitude increases with increasing in situ soil moisture measurements, contrary to expectations. An explanation could be that in these regions where the soil is relatively moist all yearlong, the surface temperature is controlled by evaporation and not by thermal inertia.

[40] For these cases, the satellite products vary as expected with the vegetation density. The passive microwaves also vary as expected with soil moisture. However, the question is: is the passive MW signal strictly correlated to the soil moisture or is it related to it through the correlation (in this case negative) between the vegetation and the soil moisture? For these locations, the vegetation

Table 4. Linear Correlation Coefficients Between the Vegetation (NDVI) and the Satellite Measurements

Variables	Total	Illinois	Iowa	Russia	India	Mongolia
Passive MW SSM/I e19V-H	−0.70	−0.72	−0.63	−0.72	−0.25	−0.83
Passive MW SSM/I e37V-H	−0.63	−0.67	−0.60	−0.65	−0.17	−0.83
Passive MW SSM/I e19V	0.06	−0.07	−0.66	0.11	−0.23	0.36
Passive MW SSM/I e19H	0.45	0.46	−0.08	0.48	−0.04	0.85
Active MW ERS small angles	0.30	−0.51	−0.10	0.26	0.49	0.60
Active MW ERS large angles	0.37	0.43	0.75	0.41	0.65	0.53
IR Ts amplitudes	−0.44	−0.49	−0.89	−0.36	−0.32	−0.76
IR normalized Ts amplitudes	−0.58	−0.74	−0.89	−0.60	−0.18	−0.80

Table 5. Linear Correlations Coefficient Between the In Situ Soil Moisture and the Satellite Measurements After Local Standardization

Variables	Total	Illinois	Iowa	Russia	India	Mongolia
Passive MW SSM/I e19V-H	0.39	0.59	0.18	0.35	0.39	−0.24
Passive MW SSM/I e37V-H	0.40	0.58	0.26	0.34	0.43	−0.20
Passive MW SSM/I e19V	−0.21	−0.29	−0.25	−0.12	−63	0.17
Passive MW SSM/I e19H	−0.35	−0.54	−0.27	−0.25	−0.61	0.27
Active MW ERS small angles	0.43	0.70	0.36	0.40	0.58	0.09
Active MW ERS large angles	0.25	−0.05	−0.04	0.24	0.71	0.00
IR Ts amplitudes	−0.01	0.12	0.08	0.05	−0.56	−0.19
IR normalized Ts amplitudes	0.12	0.31	0.17	0.17	−0.45	−0.10

density and the soil moisture are strongly anticorrelated. The passive MW polarization differences are expected to react in a similar way to an increase of soil moisture or to a decrease in vegetation. As a consequence, in these locations it is difficult to tell which parameter (vegetation or soil moisture) the passive microwaves are reacting to.

[41] Passive MW observations from SMMR along with the in situ soil moisture measurements in Illinois have already been studied intensively by *Vinnikov et al.* [1999] for 6 years (1982–1987). A rather strong correlation was found between the passive MW polarization difference at 18 GHz and the soil moisture: 0.68, very similar to what is obtained at 6.6 and 10.7 GHz from the same analysis. *Vinnikov et al.* [1999] also questioned the role of the vegetation in this correlation but the correlation they calculate between the passive MW signal and the NDVI is smaller than the correlation between the satellite signal and the soil moisture. They concluded that the MW signal is thus likely to be more sensitive to the soil moisture than to the vegetation density. We question this conclusion.

[42] From the top panels of Figure 4, for the Illinois (pluses) and Russian (asterisks) stations, it is clear that the correlation between the passive MW and the soil moisture is directly related to the correlation between the soil moisture and the vegetation: when the correlation between the vegetation and the soil moisture varies from −1 to 1, the correlation between the emissivity polarization difference and the soil moisture goes from 1 to −1, almost linearly, instead of an expected strongly positive slope. In contrast, the correlation between the passive MW and the vegetation is significant, whatever the correlation between the soil moisture and the vegetation. These results in Illinois and Russia clearly show that the passive MW polarization differences are primarily sensitive to the vegetation density, not to the soil moisture. It is worth noting that the correlation between the soil moisture and the passive MW is as good at 19 GHz as at 37 GHz and only marginally lower at 85 GHz. In contrast, the sensitivity to soil moisture is expected to decrease with increasing frequency, essentially because of increasing attenuation by vegetation. *Vinnikov et al.* [1999] were also surprised to find a comparable or even better correlation with soil moisture at 18 GHz as at 6 GHz. The passive MW correlated to the soil moisture via the correlation between the soil moisture and the vegetation explains this frequency behavior.

[43] Correlation between the T_s amplitude and the in situ soil moisture measurements also appears to be related to the correlation between vegetation and soil moisture (see Figure 4, bottom left scatterplot). In this case, a strong anticorrelation is expected between the satellite variable and the soil moisture because the thermal inertia increases with increasing soil moisture and as a consequence the T_s amplitude decreases. By the same token, vegetation also containing moisture that increases the thermal inertia, the T_s amplitude decreases with increasing vegetation density. As observed on Figure 2 (bottom scatterplots), the T_s amplitude is anticorrelated with the vegetation. When the vegetation and the soil moisture are positively correlated, the T_s amplitude and the soil moisture have the expected anticorrelation through their link to the vegetation.

3.2.2. India

[44] The study region in India is characterized by a very large seasonal cycle of soil moisture, driven by the summer monsoon: a strong relationship is observed between the in situ soil moisture and the GPCP rain estimate. The NWP soil moisture estimates agree reasonably well with the in situ measurements. The limited amplitude of the vegetation cycle and its low average value (as observed by the NDVI) contrast with the soil moisture seasonal cycle. On average, for all satellite observations (except the individual passive MW polarizations with vegetation) the correlations with the soil moisture and the vegetation have the expected signs (see Tables 3, 4, and 5). In Figure 2, several Indian cases are outliers with respect to the correlation between passive MW and soil moisture (bottom panel on the left). The presence of standing water on the surface in areas of low vegetation density could explain this particular behavior. During the wet season, for several cases (among which is the case presented in Figure 3), the polarization difference increases with increasing frequency during the wet season, which is expected from a surface of standing water. The correlation between T_s normalized amplitude and the ERS observations is strong and has the expected sign. Increasing vegetation and increasing soil moisture are expected to have the same effect on these satellite observations, as a consequence, when vegetation and soil moisture are positively correlated, their effects add and correlation with soil moisture is stronger. However, as noted, the vegetation does not vary annually as strongly as in the midlatitude regions.

3.2.3. Mongolia

[45] The soil moisture measurements are only available for 1993 during the growing season. The amplitude of the seasonal cycle of the soil moisture is small in this region as observed from in situ measurements over twenty years [*Robock et al.*, 2000]. The NWP outputs also show very stable soil moisture at the surface. The linear correlations with the soil moisture (Figure 3d) have been calculated but the number of coincidences being very limited, the figures should be considered with caution. Figure 3 and Table 3 show that all the satellite variables are very well correlated

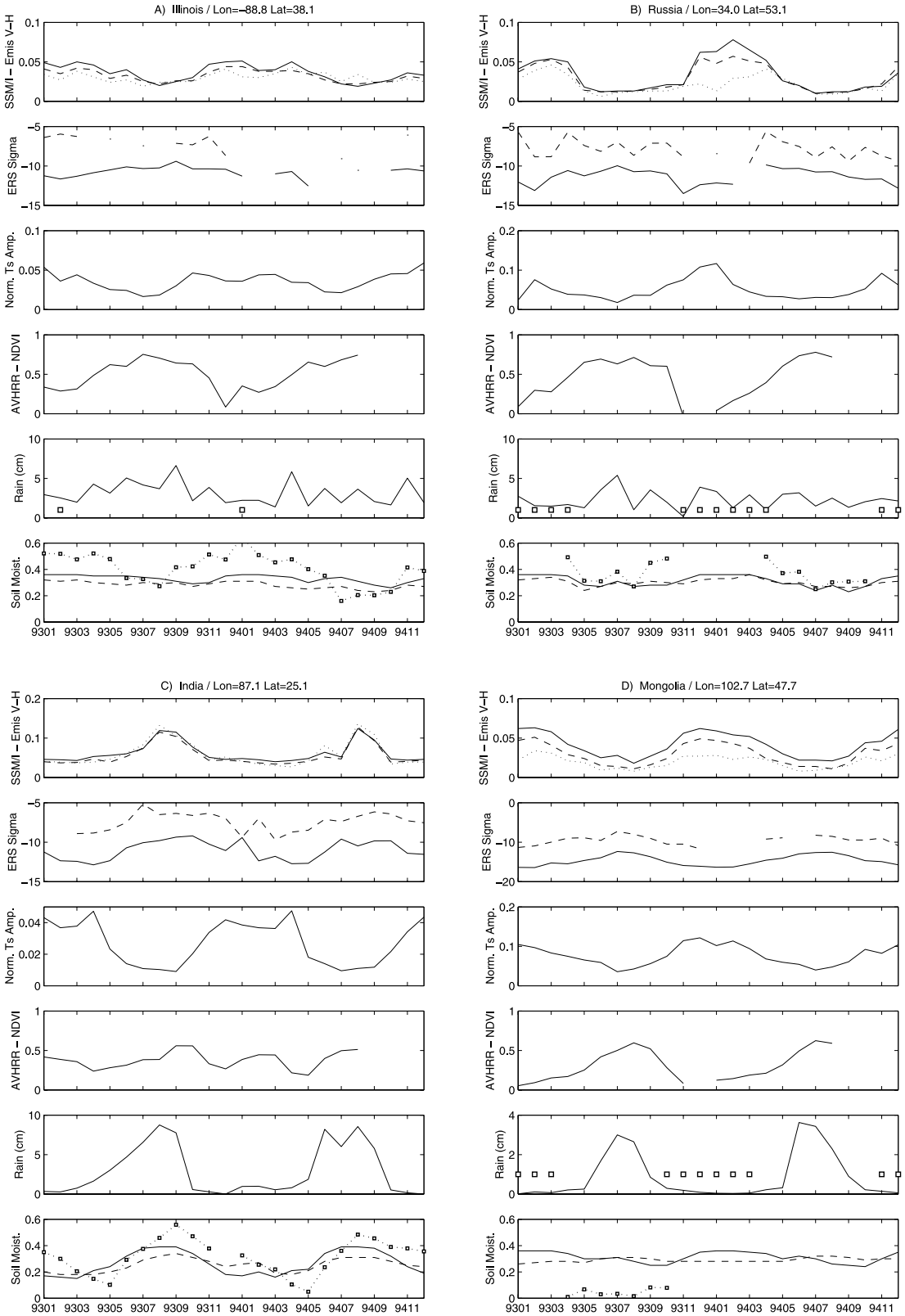

Figure 3. Time series of the satellite variables for four locations from January 1993 to December 1994, along with other surface estimates. From top to bottom for each location: the passive microwave emissivity polarization differences at 19 GHz (solid line), 37 GHz (long dash line), and 85 GHz (short dash line); the active microwave backsattering for small (dash line) and large (solid line) incidence angles; the T_s diurnal amplitude normalized by the solar flux; the NDVI; the rain rate from GPCP along with the snow flag from NOAA; and the soil moisture in situ measurements (markers and dash line) along with the top layer soil moisture from NWP models (NCEP with solid lines and ECMWF dash line).

Table 6. Linear Correlations for Each Station in Figure 3

Variable	Illinois	Russia	India	Mongolia
With In Situ Soil Moisture				
Vegetation	−0.71	−0.84	0.82	−0.07
Passive MW SSM/I e19V-H	0.85	0.76	0.66	0.15
Passive MW SSM/I e37V-H	0.84	0.74	0.68	0.15
Active MW ERS small ang.	0.70	0.84	0.71	−0.49
Active MW ERS large ang.	−0.34	0.44	0.83	−0.21
IR Norm. Ts amp.	0.32	0.20	−0.48	0.43
With NDVI Vegetation				
Passive MW SSM/I e19V-H	−0.79	−0.72	0.50	−0.93
Passive MW SSM/I e37V-H	−0.86	−0.73	0.49	−0.92
Active MW ERS small ang.les	−0.16	0.11	0.40	0.79
Active MW ERS large angles	0.30	0.77	0.65	0.96
IR normalized Ts amplitudes	−0.66	−0.61	−0.40	−0.91

with vegetation whereas limited correlation is observed with soil moisture which varies in a very narrow range (Table 4). Compared to the midlatitude regions, Mongolia represents a rather dry region with low levels of precipitation, soil moisture, and vegetation density (lower mean NDVI and mean ERS backscattering coefficients). Nevertheless, it is interesting that the same behavior is observed with respect to the correlation between satellite data and the surface characteristics (soil moisture and vegetation): in Figure 4, in Mongolia (dashes), the correlation between the passive MW and soil moisture also decreases with increasing correlation between vegetation and soil moisture. As already mentioned for the other regions, the presence of snow affects the passive MW at high frequency with a depolarization of the signal due to random scattering in the snowpack.

4. Discussion and Conclusions

[46] Today, there is no dedicated satellite mission for soil moisture retrieval. Passive MW observations at L-band from the SMOS or HYDROS satellites will offer optimum sensitivity to soil moisture after their launch in 2007 and 2010, respectively. Meanwhile, this study explores and compares the sensitivity of the available satellite measurements to the soil moisture.

[47] Three categories of satellite observations are analyzed with respect to in situ soil moisture measurements in five separate regions. Although these five regions do not cover the large variability that can be encountered over the world (for instance there are no forested cases nor semiarid ones), they still represent different soil moisture regimes. The simultaneous analysis of the various satellite observations and the large amount of in situ measurements has two major advantages.

[48] First, it helps bring out the physical processes that drive the satellite observations. For example, we clearly show that the passive MW polarization difference at 19 GHz and above is essentially sensitive to the vegetation, not to the soil moisture. This conclusion could not have been easily drawn from an analysis of in situ measurements in one region only.

[49] Second, this approach enables an objective comparison of the relative potential of the various satellite observations to indicate the soil moisture variations, when the effect of more regional differences is suppressed. Most studies have been limited to one instrument, usually with the underlying assumption that it is the best one for this purpose, so it is often very difficult to assess the relative sensitivity of the observation types to a given surface characteristic.

[50] The linear correlation coefficients that are calculated between the in situ soil moisture measurements and the available satellite variables are low when considered over all regions. Local variability of the soil moisture in situ measurements is only partly responsible for this. Vegetation effects do interfere with the soil moisture signal that is received by the satellite, to varying degrees depending on the satellite observation type. The correlation between the satellite variables and the vegetation is strong, especially for the passive MW polarization difference. We are fully aware of the limitation of the NDVI as a proxy for the vegetation, but in this study no other alternative was available. When the correlation between the soil moisture and the passive MW polarization difference is strong, it is because of the large anticorrelation between the vegetation and the soil moisture. This is why the correlation between this parameter and soil moisture is similar at 19 and 37 GHz, whereas a higher correlation at 19 GHz would be expected if it was directly sensitive to the soil moisture. Active MW observations at low incidence angle appear to be more sensitive to the soil moisture than the other satellite variables, with the observations at larger incidence angles being more sensitive to the vegetation. *Wagner et al.* [1999a] already observed this behavior with ERS measurements.

[51] In areas where the surface temperature T_s is controlled by evaporation, not by thermal inertia, the T_s diurnal amplitude extracted from the infrared observations is not well correlated with the soil moisture. However, in other regions like India, this satellite-derived information could be an indicator of soil moisture.

[52] Each satellite observation is differently sensitive to a large number of surface characteristics such as soil moisture, vegetation, soil texture, or roughness. Some of these vary strongly from region to region but not strongly at each location. Comparisons between satellite observations and in situ soil moisture measurements help decipher the complex relationships between the remotely sensed signal and the surface characteristics. We have shown capability to separate the region-to-region effects to isolate local time variations.

[53] However, the in situ soil moisture data set does not represent the whole range of variability over the globe and a global understanding cannot be directly derived from this study. To achieve this goal we try analyzing the outputs from the ECMWF and NCEP reanalyses along with the satellite variables. On the basis of the statistical analysis of the comparison between the NWP soil moisture estimates and the satellite variables in addition to the understanding gained from this study of coincident in situ measurements and satellite observations, a method can be derived to establish a statistical relationship between surface parameters such as soil moisture and satellite observations. This statistical link can be used to check the consistency between modeled soil moisture and satellite measurements. This is the objective of part 2 of this study. This same analysis can be applied to the GSWP2 results when they become available.

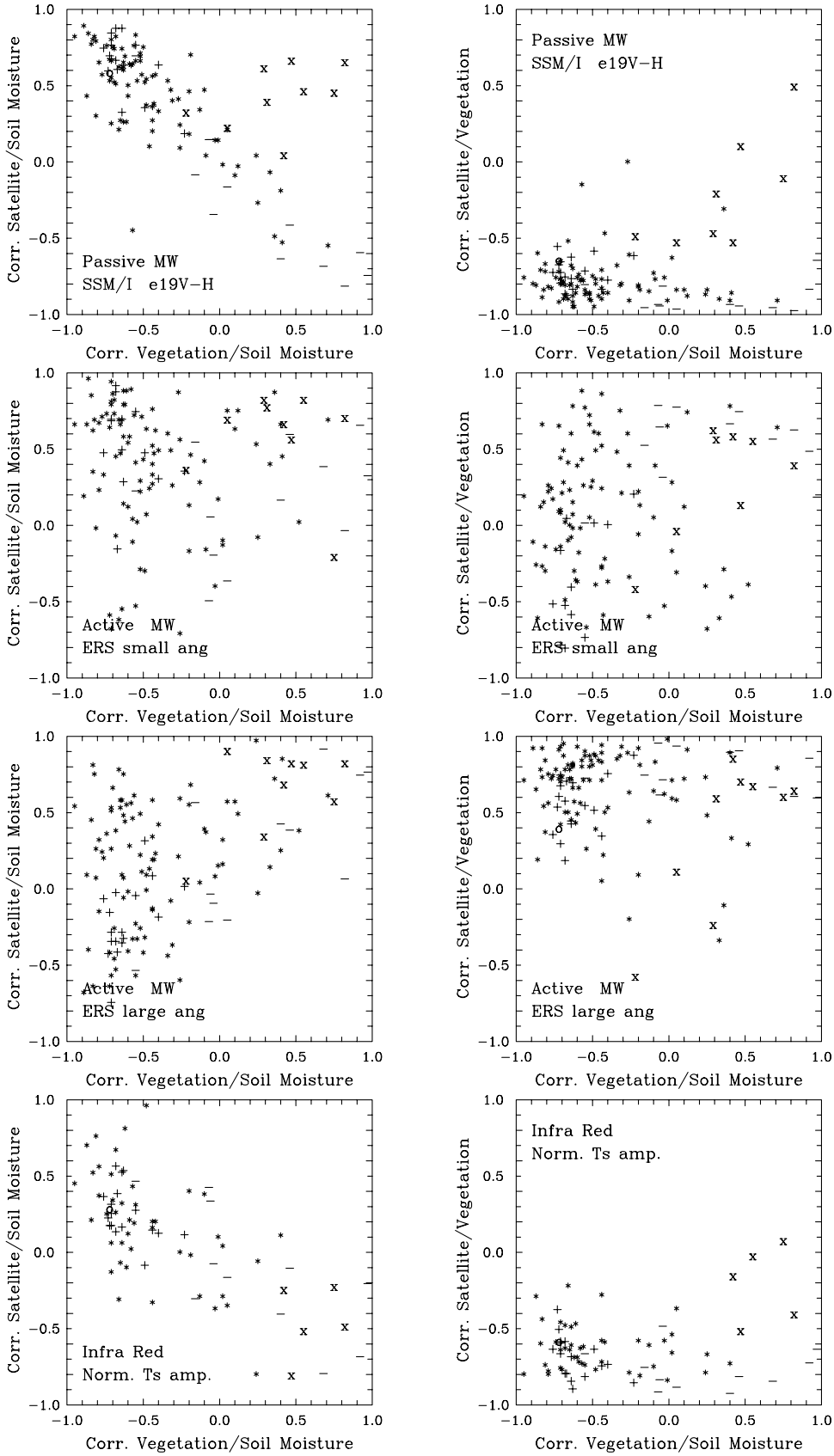

Figure 4. The correlation between the satellite variables. (left) In situ soil moisture measurements and (right) vegetation density are plotted against vegetation density (NDVI) and in situ soil moisture measurements. The satellite variable considered is indicated in each box. Symbols represent each region: pluses, Illinois; circles, Iowa; asterisks, Russia; crosses, India; dashes, Mongolia.

[54] **Acknowledgments.** We would like to thank Hervé Douville from Météo-France for fruitful discussions and Ralph Karow for his help in data processing. We are grateful to two anonymous reviewers for their careful reading of the manuscript and constructive comments. We thank Jean-Christophe Calvet and Jean-Pierre Wigneron for the MUREX and PORTOS soil moisture profiles. The ERS scatterometer data have been provided by IFREMER. This work was partly supported by the NASA Radiation Sciences and Hydrology Programs, and by NOAA grant NA03-OAR-4310057.

References

Aires, F., C. Prigent, W. B. Rossow, and M. Rothstein (2001), A new neural network approach including first-guess for retrieval of atmospheric water vapor, cloud liquid water path, surface temperature and emissivities over land from satellite microwave observations, *J. Geophys. Res.*, *106*, 14,887–14,907.

Aires, F., C. Prigent, and W. B. Rossow (2004), Temporal interpolation of global surface skin temperature diurnal cycle over land under clear and cloudy conditions, *J. Geophys. Res.*, *109*, D04313, doi:10.1029/2003JD003527.

Basist, A., N. C. Grody, T. C. Peterson, and C. N. Williams (1998), Using the Special Sensor Microwave/Imager to monitor land surface temperatures, wetness, and snow cover, *J. Atmos. Sci.*, *37*, 888–911.

Begue, A., and R. Myneni (1996), Operational relationships between NOAA-advanced very high resolution radiometer vegetation indices and daily fraction of absorbed photosynthetically active radiation, established for Sahelian vegetation canopies, *J. Geophys. Res.*, *101*, 21,275–21,289.

Calvet, J.-C., A. Chanzy, and J.-P. Wigneron (1996), Surface temperature and soil moisture retrieval in the Sahel from airborne multifrequency microwave radiometry, *IEEE Trans. Geosci. Remote Sens.*, *34*, 588–599.

Calvet, J. C., et al. (1999), MUREX: A land-surface field experiment to study the annual cycle of the energy and water budgets, *Ann. Geophys.*, *17*, 838–854.

Choudhury, B. J. (1989), Monitoring global land surface using Nimbus-7 37 GHz data: Theory and examples, *Int. J. Remote Sens.*, *10*, 1579–1605.

Choudhury, B. J., and C. J. Tucker (1987), Monitoring global vegetation using Nimbus-7 37 GHz data: Some empirical relations, *Int. J. Remote Sens.*, *8*, 1837–1868.

DeFries, R. S., J. R. G. Townshend, and M. C. Hansen (1999), Continuous fields of vegetation characteristics at the global scale at 1-km resolution, *J. Geophys. Res.*, *104*, 16,911–16,923.

De Ridder, K. (2003), Surface soil moisture monitoring over Europe using Special Sensor Microwave/Imager (SSM/I) imagery, *J. Geophys. Res.*, *108*(D2), 4422, doi:10.1029/2002JD002796.

Douville, H., E. Bazile, P. Caille, D. Giard, J. Noilhan, L. Peirone, and F. Taillefer (1999), Global soil wetness project: Forecast and assimilation experiment performed at Météo-France, *J. Meteorol. Soc. Jpn.*, *77*, 305–316.

Du, Y., F. T. Ulaby, and M. G. Dobson (2000), Sensitivity to soil moisture by active and passive microwave sensors, *IEEE Trans. Geosci. Remote Sens.*, *38*, 105–114.

Entekhabi, D., E. Njoku, and P. Houser (2002), The Hydrosphere State (HYDROS) mission approach to high resolution and frequent revisit data products for hydrometeorological and hydroclimatological applications, *Eos Trans. AGU*, *83*(47), Fall Meet. Suppl., Abstract H72A-0845.

Entin, J. K., A. Robock, K. Y. Vinnikov, V. Zabelin, S. Liu, A. Namkhai, and T. Adyasuren (1999), Evaluation of global soil wetness project soil moisture simulations, *J. Meteorol. Soc. Jpn.*, *77*, 183–198.

Entin, J. K., A. Robock, K. Y. Vinnikov, S. E. Hollinger, S. Liu, and A. Namkhai (2000), Temporal and spatial scales of observed soil moisture variations in the extratropics, *J. Geophys. Res.*, *105*, 11,865–11,877.

Friedl, M. A. (1995), Modeling land surface fluxes using a sparse canopy model and radiometric surface temperature measurements, *J. Geophys. Res.*, *100*, 25,435–25,446.

Frison, P.-L., and E. Mougin (1996a), Use of ERS-1 wind scatterometer data over land surfaces, *IEEE Trans. Geosci. Remote Sens.*, *34*, 550–560.

Frison, P.-L., and E. Mougin (1996b), Monitoring global vegetation dynamics with ERS-1 wind scatterometer data, *Int. J. Remote Sens.*, *17*, 3201–3218.

Gillies, R. R., and T. N. Carlson (1995), Thermal remote sensing of surface soil water content with partial vegetation cover for incorporation into climate model, *J. Appl. Meteorol.*, *3*, 745–756.

Goetz, S. J. (1997), Multi-sensor analysis of NDVI, surface temperature and biophysical variables at a mixed grassland site, *Int. J. Remote Sens.*, *8*, 71–94.

Goetz, S. J. (2002), Recent advances in remote sensing of biophysical variables: An overview of the special issue, *Remote Sens. Environ.*, *79*, 145–146.

Gutman, G. G. (1999), On the use of long-term global data of land reflectances and vegetation indices from the advanced very high resolution radiometer, *J. Geophys. Res.*, *104*, 6241–6255.

Hollinger, S. E., and A. I. Scott (1994), A soil moisture climatology of Illinois, *J. Clim.*, *7*, 822–833.

Hollinger, J. P., R. Lo, G. Poe, R. Savage, and J. Pierce (1987), Special Sensor Microwave/Imager user's guide, Nav. Res. Lab., Washington, D.C.

Huffman, G. J. (Ed.) (1997), The Global Precipitation Climatology Project monthly mean precipitation data set, *WMO/TD Rep. 808*, 37 pp., World Meteorol. Org., Geneva.

Jackson, T. J., and A. Y. Hsu (2001), Soil moisture and TRMM microwave imager relationship in the Southern Great Plains 1999(SGP99) experiment, *IEEE Trans. Geosci. Remote Sens.*, *39*, 1632–1642.

Jin, M. (2004), Analysis of land skin temperature using AVHRR observations, *Bull. Am. Meteorol. Soc.*, doi:10.1175/BULL.AM.METEOROL.SOC.-85-4-587.

Kalnay, E., et al. (1996), The NCEP/NCAR 40-year reanalysis project, *Bull. Am. Meteorol. Soc.*, *77*, 437–470.

Kerr, Y. H., P. Waldteufel, J.-P. Wigneron, J.-M. Martinuzzi, J. Font, and M. Berger (2001), Soil moisture retrieval from space: The Soil Moisture and Ocean Salinity (SMOS) mission, *IEEE Trans. Geosci. Remote Sens.*, *39*, 1729–1735.

Lakshmi, V., E. F. Wood, and B. J. Choudhury (1997), A soil-canopy-atmosphere model for use in satellite microwave remote sensing, *J. Geophys. Res.*, *102*, 6911–6927.

Li, H., A. Robock, S. Liu, X. Mo, and P. Viterbo (2005), Evaluation of reanalysis soil moisture simulations using updated chinese soil moisture observations, *J. Hydrometeorol.*, in press.

McFarland, M. J., R. L. Miller, and C. M. U. Neale (1990), Land surface temperature derived from the SSM/I passive microwave brightness temperatures, *IEEE Trans. Geosci. Remote Sens.*, *28*, 839–845.

Messeh, M. A., and S. Quegan (2000), Variability in ERS scatterometer measurements over land, *IEEE Trans. Geosci. Remote Sens.*, *38*, 1767–1776.

Moran, M. S., D. C. Hymer, J. Qi, and E. E. Sano (2000), Soil moisture evaluation using multi-temporal synthetic aperture radar (SAR) in a semi-arid range land, *Agric. For. Meteorol.*, *105*, 69–80.

Moulin, S., L. Kergoat, N. Viovy, and G. Dedieu (1997), Global-scale assessment of vegetation phenology using NOAA/AVHRR satellite, *J. Clim.*, *10*, 1154–1170.

Njoku, E. G. (1995), Surface temperature estimation over land using satellite microwave radiometry, in *Passive Microwave Remote Sensing of Land-Atmosphere Interaction*, edited by B. J. Choudhury et al., pp. 509–530, VSP, Utrecht, Netherlands.

Prigent, C., W. B. Rossow, and E. Matthews (1997), Microwave land surface emissivities estimated from SSM/I observations, *J. Geophys. Res.*, *102*, 21,867–21,890.

Prigent, C., W. B. Rossow, and E. Matthews (1998), Global maps of microwave land surface emissivities: Potential for land surface characterization, *Radio Sci.*, *33*, 745–751.

Prigent, C., F. Aires, W. B. Rossow, and E. Matthews (2001), Joint characterization of vegetation by satellite observations from visible to microwave wavelength: A sensitivity analysis, *J. Geophys. Res.*, *106*, 20,665–20,685.

Quesney, A., S. Le Hegarat-Mascle, O. Taconet, D. Vidal-Madjar, J.-P. Wigneron, C. Loumagne, and M. Normand (2000), Estimation of watershed soil moisture index from ERS/SAR data, *Remote Sens. Environ.*, *72*, 290–303.

Reichle, R. H., R. D. Koster, J. Dong, and A. A. Berg (2004), Global soil moisture from satellite observations, land surface models, and ground data: Implication for data assimilation, *J. Hydrometeorol.*, *5*, 430–442.

Robock, A., K. Y. Vinnikov, C. A. Schlosser, N. A. Speranskaya, and Y. Xue (1995), Use of midlatitude soil moisture and meteorological observations to validate soil moisture simulations with biosphere and bucket models, *J. Clim.*, *8*, 15–35.

Robock, A., C. A. Schlosser, K. Y. Vinnikov, N. A. Speranskaya, J. Entin, and S. Qiu (1998), Evaluation of AMIP soil moisture simulations, *Global Planet. Change*, *19*, 181–208.

Robock, A., K. Y. Vinnikov, G. Srinivasan, J. K. Entin, S. E. Hollinger, N. A. Speranskaya, S. Liu, and A. Namkhai (2000), The Global Soil Moisture Data Bank, *Bull. Am. Meteorol. Soc.*, *81*, 1281–1299.

Rossow, W. B., and R. A. Schiffer (1999), Advances in understanding clouds from ISCCP, *Bull. Am. Meteorol. Soc.*, *80*, 2261–2287.

Schmugge, T. J., T. J. Jackson, and H. L. McKim (1980), Survey of methods for soil moisture determination, *Water Resour. Res.*, *16*, 961–979.

Schmugge, T. J., W. P. Kustas, J. C. Ritchie, T. J. Jackson, and A. Rango (2002), Remote sensing in hydrology, *Adv. Water Resour.*, *25*, 1367–1385.

Srinivasan, G., A. Robock, J. K. Entin, L. Luo, K. Y. Vinnikov, P. Viterbo, and Participating AMIP Modeling Groups (2000), Soil moisture simulations in the revised AMIP models, *J. Geophys. Res.*, *105*, 26,635–26,644.

Taconet, O., R. Bernard, and D. Vidal-Madjar (1986), Evaluation of a surface/vegetation parameterization using satellite measurements of surface temperature, *J. Clim. Appl. Meteorol.*, *25*, 1752–1767.

Tanré, D., B. N. Holben, and Y. F. Kaufman (1992), Atmospheric correction algorithm for NOAA-AVHRR products: Theory and application, *IEEE Trans. Geosci. Remote Sens.*, *30*, 231–248.

Tucker, C. J., J. R. G. Townshend, and T. E. Goff (1985), African land-cover classification using satellite data, *Science*, *227*, 369–375.

Vinnikov, K. Y., and I. B. Yeserkepova (1991), Soil moisture: Empirical data and model results, *J. Clim.*, *4*, 66–79.

Vinnikov, K. Y., A. Robock, N. A. Speranskaya, and C. A. Schlosser (1996), Scales of temporal and spatial variability of midlatitude soil moisture, *J. Geophys. Res.*, *101*, 7163–7174.

Vinnikov, K. Y., A. Robock, S. Qiu, J. K. Entin, M. Owe, B. J. Choudhury, S. E. Hollinger, and E. G. Njoku (1999), Satellite remote sensing of soil moisture in Illinois, United States, *J. Geophys. Res.*, *104*, 4145–4168.

Wagner, W., J. Noll, M. Borgeaud, and H. Rott (1999a), Monitoring soil moisture over the Canadian prairies with the ERS scatterometer, *IEEE Trans. Geosci. Remote Sens.*, *37*(2), 206–216.

Wagner, W., G. Lemoine, and M. Borgeaud (1999b), A study of vegetation cover effects on ERS scatterometer data, *IEEE Trans. Geosci. Remote Sens.*, *37*, 938–947.

Wagner, W., K. Scipal, C. Pathe, D. Gerten, W. Lucht, and B. Rudolf (2003), Evaluation of the agreement between the first global remotely sensed soil moisture data with model and precipitation data, *J. Geophys. Res.*, *108*(D19), 4611, doi:10.1029/2003JD003663.

Wen, J., and Z. Su (2003), A time series based method for estimating relative soil moisture with ERS wind scatterometer data, *Geophys. Res. Lett.*, *30*(7), 1397, doi:10.1029/2002GL016557.

Wetzel, P. J., D. Atlas, and R. H. Woodward (1984), Determining soil moisture from geosynchronous satellite infrared data: A feasibility study, *J. Clim. Appl. Meteorol.*, *23*, 375–391.

Wigneron, J.-P., A. Chanzy, J.-C. Calvet, and N. Bruguier (1995), A simple algorithm to retrieve soil moisture and vegetation biomass using passive microwave measurements over crop fields, *Remote Sens. Environ.*, *51*, 331–341.

Wismann, V. (1999), A database of global C-band NRCS derived from ERS scatterometer data, *IEEE Geosci. Remote Sens. Newslett.*, *106*, 7–9.

Wismann, V., A. Cavanie, D. Hoekmann, I. Woodhouse, K. Boehnke, and C. Schmullius (1996), Land observations using ERS-1 scatterometer, *ESA Contract 11103/94/NL/CL*, Eur. Space Ag., Paris.

Woodhouse, I. H., and D. H. Hoekman (2000a), A model-based determination of soil moisture trends in Spain with the ERS scatterometer, *IEEE Trans. Geosci. Remote Sens.*, *38*, 1783–1793.

Woodhouse, I. H., and D. H. Hoekman (2000b), Determining land surface parameters from the ERS wind scatterometer, *IEEE Trans. Geosci. Remote Sens.*, *38*, 127–140.

Zhang, Y., W. B. Rossow, A. A. Lacis, V. Oinas, and M. I. Mishchenko (2004), Calculation of radiative fluxes from the surface to top of atmosphere based on ISCCP and other global data sets: Refinements of the radiative transfer model and the input data, *J. Geophys. Res.*, *109*, D19105, doi:10.1029/2003JD004457.

F. Aires, Department of Applied Physics and Applied Mathematics, Columbia University, NASA Goddard Institute for Space Studies, 2880 Broadway, New York, NY 10025, USA. (faires@giss.nasa.gov)

C. Prigent, CNRS, LERMA, Observatoire de Paris, 61 Avenue de l'Observatoire, Paris F-75014, France. (catherine.prigent@obspm.fr)

A. Robock, Department of Environmental Sciences, Rutgers University, 14 College Farm Road, New Brunswick, NJ 08901, USA. (robock@envsci.rutgers.edu)

W. B. Rossow, NASA Goddard Institute for Space Studies, 2880 Broadway, New York, NY 10025, USA. (wrossow@giss.nasa.gov)